



Synthesis, electrochemical and spectroelectrochemical characterization of novel soluble phthalocyanines bearing chloro and quaternizable bulky substituents on peripheral positions

H.R. Pekbelgin Karaoğlu^a, Atif Koca^b, Makbule Burkut Koçak^{a,*}

^a Department of Chemistry, Istanbul Technical University, TR34469 Maslak, Istanbul, Turkey

^b Chemical Engineering Department, Engineering Faculty, Marmara University, TR 34722 Göztepe, Istanbul, Turkey

ARTICLE INFO

Article history:

Received 2 June 2011

Received in revised form

22 July 2011

Accepted 27 July 2011

Available online 5 August 2011

Keywords:

Phthalocyanine

Diethylaminophenoxy

Water-soluble

Aggregation behavior

Electrochemistry

Spectroelectrochemistry

ABSTRACT

A new phthalonitrile derivative (**2**), bearing diethylaminophenoxy – and chloro-substituents at peripheral positions was synthesized in this work. Cyclotetramerization of (**2**) in hexanol gave the desired metal-free (**4**) and metallophthalocyanines (**5–8**). These new phthalocyanines (**4–8**) were converted into water-soluble quaternized products by the reaction with methyl iodide (**9–11**). The novel compounds have been characterized by using elemental analysis, UV–Vis, FT-IR, ¹H NMR and MS spectroscopic data. The aggregation behaviors of the phthalocyanine complexes were studied in different solvents and concentrations. Electrochemical and spectroelectrochemical characterization of the complexes were also performed in solution. Cobalt phthalocyanine gives both metal-based and ring-based reduction processes in comparison to the complexes having 2H⁺, Zn²⁺, Ni²⁺ and Cu²⁺ metal center which give only ring-based reduction processes. Electrochemical and spectroelectrochemical measurements exhibit that all complexes oxidatively electro-polymerize on the Pt working electrode during repetitive cyclic voltammetry measurements. An in-situ electrocolorimetric method was applied to investigate the color of the electrogenerated anionic and cationic forms of the complexes for possible electrochromatic applications.

© 2011 Elsevier Ltd. All rights reserved.

1. Introduction

Phthalocyanines (Pcs) are interesting class of compounds which exhibit unique optical, electronic, catalytic and structural properties [1]. These unique properties lead to a great interest in different scientific and technological areas such as photo-conducting agents in photocopying devices, chemical sensors, molecular metals, liquid crystals, non-linear optics and catalysis [1–3]. In recent years, phthalocyanines have also been successfully used in photodynamic therapy of cancer (PDT) due to their intense absorption in the red region (600–800 nm) of the optical spectrum [4–9]. For such applications a good solubility in polar solvents is preferred [4,10–13].

Applications of peripherally unsubstituted metal-free and metallophthalocyanines are limited due their insolubility in most organic solvents and aqueous media. Phthalocyanines possess a large conjugated π -system which leads π -stacking (aggregation)

between planar macrocycles, which provides decreasing in the distances between the macrocycles. The solubility of phthalocyanines can be improved by introducing of substituents on the periphery of the molecule, since these substituents increase the distance between the stacked phthalocyanines [14–29]. The size and the nature of the substituents are not the only criteria for the solubility of the substituted phthalocyanines; the change in symmetry caused by the substituents is also important. Usually, tetra-substituted phthalocyanines (Pcs) are more soluble than corresponding octa-substituted Pcs due to the formation of four constitutional isomers and the high dipole moment that results from the unsymmetrical arrangement of the substituents on the periphery [1,17–22]. In this sense, octa-substituted phthalocyanines were obtained from disubstituted phthalonitrile derivatives with two different substituents in the 4- and 5- positions, have been expected to show similar behavior. This new class of octa-substituted phthalocyanines is relatively less reported, only a few well characterized species are known [23–29]. In previous papers, we described the synthesis of these types of phthalocyanines [26–28]. In addition, we investigated the reactivity of remaining chloro group in newly synthesized phthalonitrile to obtain other

* Corresponding author. Tel.: +90 212 285 69 64; fax: +90 212 285 63 86.

E-mail address: mkocak@itu.edu.tr (M. B. Koçak).

sophisticated differently substituted phthalonitriles such as bearing bulky diethylmalonate and alkylsulfanyl [27] or dimethylaminoethylsulfanyl groups [28] at 4- and 5-positions.

In the present paper, we describe the synthesis and characterization of novel phthalocyanines bearing four chloro and four bulky dialkylaminophenoxy or trialkylaminophenoxy substituents on the peripheral positions. The latter group was designed to achieve solubility in water and DMSO [30–36]. The functions of metallophthalocyanine derivatives are almost exclusively based on their electron transfer reactions because of the π -electron-conjugated ring system periphery of the molecule. It is necessary to examine the electron transfer behavior of newly synthesized phthalocyanine complexes in solution in order to study further applications such as chemical sensors, electrocatalysts, and electrochromic materials. Therefore, in this study, we have also examined the voltammetric and spectroelectrochemical properties of these novel phthalocyanines.

2. Experimental

2.1. Chemicals and instrumentation

IR spectra were recorded on a Perkin Elmer Spectrum One FT-IR (ATR sampling accessory) spectrophotometer, electronic spectra on a Scinco S-3100 spectrophotometer. ^1H NMR spectra were recorded on Bruker 250 MHz using TMS as internal standard. Mass spectra were measured on a Micromass Quattro LC/ULTIMA LC-MS/MS spectrometer. All reagents and solvents were of reagent grade quality obtained from commercial suppliers. The homogeneity of the products was tested in each step by TLC. The solvents were stored over molecular sieves. Anhydrous potassium carbonate (K_2CO_3) and sodium carbonate (Na_2CO_3) were finely ground and dried at 100 °C. 1,2-Dichloro-4,5-dicyanobenzene (**1**) was prepared according to reported procedure [37].

2.2. Electrochemical in-situ spectroelectrochemical and in-situ electrocolorimetric measurements

The cyclic voltammetry (CV) and square wave voltammetry (SWV) measurements were carried out with Gamry Reference 600 potentiostat/galvanostat controlled by an external PC and utilizing a three-electrode configuration at 25 °C. The working electrode was a Pt disc with a surface area of 0.071 cm². A Pt wire served as the counter electrode. Saturated calomel electrode (SCE) was employed as the reference electrode and separated from the bulk of the solution by a double bridge. Electrochemical grade TBAP in extra pure DCM was employed as the supporting electrolyte at a concentration of 0.10 mol dm⁻³.

UV–Vis absorption spectra and chromaticity diagrams were measured by an Ocean Optics QE65000 diode array spectrophotometer. In-situ spectroelectrochemical measurements were carried out by utilizing a three-electrode configuration of thin-layer quartz thin-layer spectroelectrochemical cell at 25 °C. The working electrode was a Pt gauze semitransparent electrode. Pt wire counter electrode separated by a glass bridge and a SCE reference electrode separated from the bulk of the solution by a double bridge were used. In-situ electrocolorimetric measurements, under potentiostatic control, were obtained using an Ocean Optics QE65000 diode array spectrophotometer at color measurement mode by utilizing a three-electrode configuration of thin-layer quartz spectroelectrochemical cell. The standard illuminant A with 2° observer at constant temperature in a light booth designed to exclude external light was used. Prior to each set of measurements, background color coordinates (x , y , and z values) were taken at open-circuit, using the electrolyte solution without

the complexes under study. During the measurements, readings were taken as a function of time under kinetic control, however only the color coordinates at the beginning and final of each redox processes were reported.

2.3. Synthesis

2.3.1. 1-Chloro-3,4-dicyano-6-[3-(diethylamino)phenoxy]benzene (**2**)

1,2-Dichloro-4,5-dicyanobenzene (**1**) (0.50 g, 2.50 mmol) was dissolved in 10.0 cm³ dry DMF at 50 °C, and 3-(diethylamino)phenol (0.83 g, 5.00 mmol) was added to this solution. After stirring for 15 min, 1.07 g of finely ground anhydrous Na_2CO_3 (10 mmol) was added portion wise during 2 h with efficient stirring. The reaction mixture was stirred under nitrogen at 50 °C for further 96 h. After being cooled to room temperature, the mixture was poured into ice/water (100 cm³). The resulting deep brown solid was collected by filtration and washed with water until the washings were neutral. The solid was dissolved in AcOEt and washed several times with aqueous 1 M NaOH and with brine. The organic solution was dried with Na_2SO_4 and the solvent was evaporated to give the crude product. Finally pure product was obtained by chromatography on silica gel stationary phase with CHCl_3 :*n*-hexane (5:1) mixture as eluent. The final product (**2**) was soluble in THF, CHCl_3 , DMF, and DMSO. Yield: 0.21 g (31%). ^1H NMR (CDCl_3): δ 7.87 (s, H–Ar), 7.26 (t, H–Ar), 7.13 (s, H–Ar), 6.59 (dd, H–Ar), 6.30 (t, H–Ar), 6.24 (dd, H–Ar), 3.35 (q, O–CH₂), 1.17 (t, CH₃); IR (ν , cm⁻¹): 3077 (H–Ar), 2963, 2926 (H–Aliphatic), 2236 (C≡N), 1565 (Ar C=C), 1272 (Ar C–N), 1247 (Ar–O–Ar); ^{13}C NMR (CDCl_3): δ 158.78, 154.4, 150.2, 135.03, 131.1, 128.8, 120.5, 115.5, 114.6, 109.7, 105.7, 106.0, 102.8, 44.36, 12.31; Elemental analysis: $\text{C}_{18}\text{H}_{16}\text{ClN}_3\text{O}$ calculated %: C, 66.36; H, 4.95; Cl, 10.88; N, 12.90; O, 4.91; found %: C, 66.48; H, 5.21; N, 13.09; MS [m/z]: 324 [$\text{M} - \text{H}$]⁺, 290 [$\text{M} - \text{Cl}$]⁺. m.p.: 149.4 °C.

2.3.2. 1,2-Dicyano-4,5-bis[3-(diethylamino)phenoxy]benzene (**3**)

The compound **3** was prepared following the procedure described for **2** starting from **1** (0.83 g, 5.00 mmol) and 3-(diethylamino)phenol (0.83 g, 5.00 mmol) in 10 cm³ DMF using K_2CO_3 instead of Na_2CO_3 as a base. The crude product was precipitated by pouring the reaction mixture into copious amount of water and was purified by recrystallization from ethanol. The compound **3** was soluble in THF, CHCl_3 , CH_2Cl_2 , DMF, and DMSO. Yield: 25%. ^1H NMR (CDCl_3): δ 7.83 (s, H–Ar), 7.21 (t, H–Ar), 7.12 (s, H–Ar), 6.56 (dd, H–Ar), 6.33 (t, H–Ar), 6.25 (dd, H–Ar), 3.34 (q, O–CH₂), 1.16 (t, CH₃); ^{13}C NMR (CDCl_3): δ 158.55, 154.57, 150.01, 135.26, 131.14, 120.33, 109.72, 108.87, 106.03, 103.18, 44.44, 12.49; IR (ν , cm⁻¹): 3076 (H–Ar), 2965, 2928 (H–Aliphatic), 2234 (C≡N), 1564 (Ar C=C), 1272 (Ar C–N), 1247 (Ar–O–Ar); $\text{C}_{28}\text{H}_{30}\text{N}_4\text{O}_2$ calculated %: C, 73.98; H, 6.65; N, 12.33; O, 7.04; found %: C, 74.12; H, 6.82; N, 12.39; MS [m/z]: 454 [M]⁺, 439 [$\text{M} - \text{CH}_3$]⁺, 425 [$\text{M} - \text{CH}_3 - \text{CH}_3$]; m.p.: 137.5 °C.

2.4. General procedures for phthalocyanine derivatives (**4**–**9**)

Reaction: A mixture of compound **2** (97.7 mg, 0.3 mmol), 0.075 mmol anhydrous metal salts [CoCl_2 , 9.7 mg; NiCl_2 , 9.7 mg; CuCl_2 , 10.1 mg; $\text{Zn}(\text{CH}_3\text{COO})_2$, 13.7 mg; NiCl_2 , 9.5 mg] and catalytic amount of DBU (1,8-diazabicyclo[5.4.0]undec-7-ene) in 2.0 cm³ of hexan-1-ol was heated with stirring at 160 °C in a sealed glass tube (10 × 75 mm) for 24 h under nitrogen. For metal-free phthalocyanine no metal salt was required. After cooling to room temperature the green suspension was precipitated with methanol, filtered, washed with the same solvent, and finally dried *in vacuo*. **Purification:** chromatography. **Colors:** Dark green. **Solubility:** Extremely soluble in CHCl_3 , THF, DMF and DMSO.

2.4.1. 2,9,16,23-Tetrakis-[3-(diethylamino)phenoxy]-3,10,17,24-tetrachloro-phthalocyanine (4)

The purification of the crude product was performed by column chromatography on silica gel (CHCl₃ and Hexane 10:1 v/v). Pure compound **4** was obtained as an isomeric mixture. Yield: 43 mg, 44%; IR, γ_{\max} (cm⁻¹): 3288 (N–H), 3088–3032 (C–H, aromatic) 2967–2925 (C–H aliphatic), 1262–1242 (Ar–O–Ar); UV–Vis (CHCl₃): λ_{\max} (nm) (log ϵ) = 343 (5.04), 670 (5.18), 705 (5.22); ¹H NMR (CDCl₃ δ): 8.39–7.92, 7.25–7.31, 6.76–6.54 (ms, Ar–H, 24H), 3.45–3.43 (m, N–CH₂, 16H), 1.28–1.21 (m, CH₃, 24H), –5.35 (br s, NH, 2H) ppm; elemental analysis: C₇₂H₆₆Cl₄N₁₂O₄ calculated %: C, 66.25; H, 5.10; Cl, 10.87; N, 12.88; O, 4.90; found %: C, 66.37; H, 5.19; N, 13.03; MS: (ESI) yielded an isotopic cluster peak at m/z 1305.5 [M]⁺.

2.4.2. 2,9,16,23-Tetrakis-[3-(diethylamino)phenoxy]-3,10,17,24-tetrachloro-phthalocyaninato)copper (II) (5)

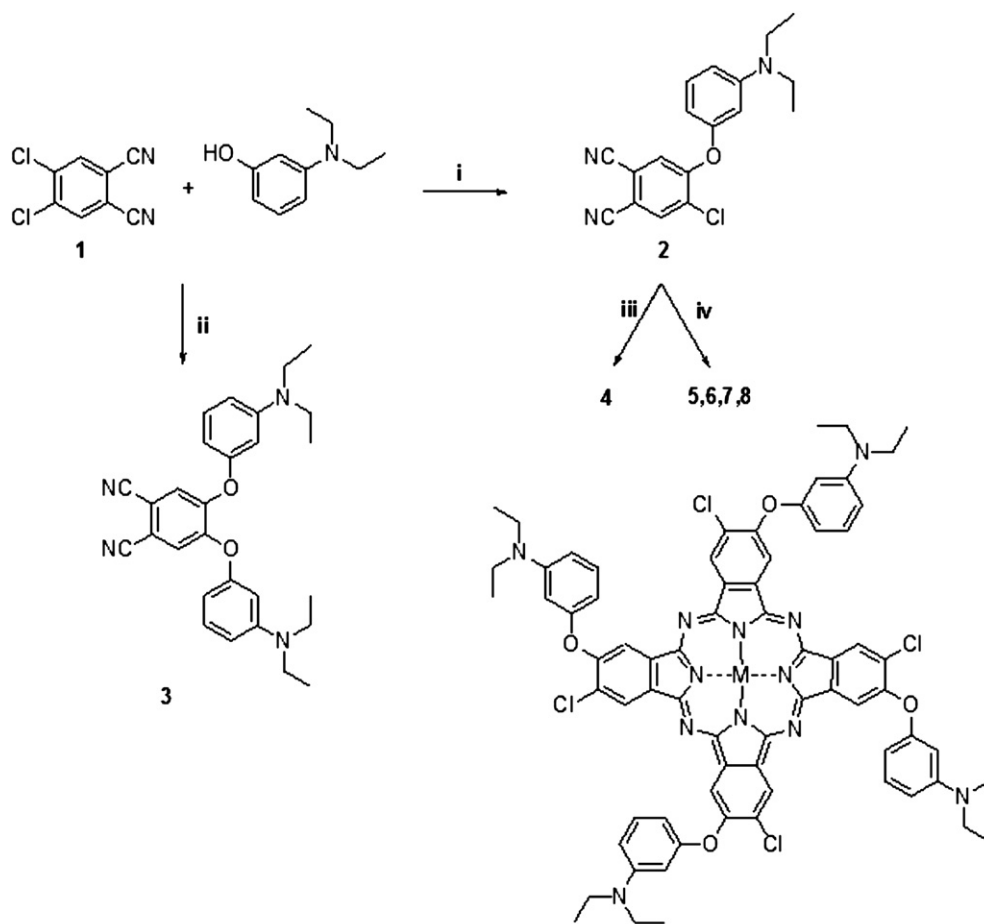
The purification was performed similarly to **4**, the pure product **5** was obtained as an isomeric mixture. Yield: 41 mg, 40%; IR, γ_{\max} (cm⁻¹): 3075–3057 (C–H, aromatic) 2964–2919 (C–H aliphatic), 1273–1242 (Ar–O–Ar); UV–Vis (CHCl₃): λ_{\max} (nm) (log ϵ) = 342 (4.90), 623 (4.77), 684 (5.02); C₇₂H₆₄Cl₄CuN₁₂O₄ calculated %: C, 63.27; H, 4.72; Cl, 10.38; N, 12.30; O, 4.68; Cu, 4.65; found %: C, 63.35; H, 4.75; N, 12.42%; MS: (ESI) yielded an isotopic cluster peak at m/z 1365.7 [M – H]⁺.

2.4.3. 2,9,16,23-Tetrakis-[3-(diethylamino)phenoxy]-3,10,17,24-tetrachloro-phthalocyaninato)cobalt (II) (6)

The purification of the crude product was performed by column chromatography on silica gel as the stationary phase using CHCl₃ as eluent, which gave pure compound **6** as an isomeric mixture. Yield: 63.5 mg, 62%; IR, γ_{\max} (cm⁻¹): 3075 (C–H, aromatic) 2966–2926 (C–H aliphatic), 1272–1241 (Ar–O–Ar); UV–Vis (CHCl₃): λ_{\max} (nm) (log ϵ) = 308 (5.02), 616 (4.69), 673 (5.16); C₇₂H₆₄Cl₄N₁₂O₄Co calculated %: C, 63.48; H, 4.74; Cl, 10.41; N, 12.34; O, 4.70; Co, 4.33; found %: C, 63.63; H, 4.82; N, 12.47; MS: (ESI) yielded an isotopic cluster peak at m/z 1362.3 [M]⁺.

2.4.4. 2,9,16,23-Tetrakis-[3-(diethylamino)phenoxy]-3,10,17,24-tetra-chloro-phthalocyaninato}zinc (II) (7)

The purification was performed similarly to **6**, the pure product **7** was obtained as an isomeric mixture. Yield: 41 mg, 40%; IR, γ_{\max} (cm⁻¹): 3075(C–H, aromatic), 2965–2924 (C–H aliphatic), 1272–1239 (Ar–O–Ar); UV–Vis (CHCl₃): λ_{\max} (nm) (log ϵ) = 355 (4.72), 654 (4.76); ¹H NMR (CDCl₃ δ): 7.87–7.47, 6.97–6.93, 6.33–6.29 (ms, Ar–H, 24H), 3.21 (br s, N–CH₂, 16H), 1.15–1.09 (m, CH₃–24H) ppm; C₇₂H₆₄Cl₄N₁₂O₄Zn calculated %: C, 63.19; H, 4.71; Cl, 10.36%; N, 12.28%; O, 4.68; Zn, 4.78% found %: C, 63.31; H, 4.78; N, 12.35%; MS: (ESI) yielded an isotopic cluster peak at m/z 1369.5 [M + H]⁺.



Scheme 1. Synthesis of Pcs **4–8**. i. Na₂CO₃, DMF, 50 °C, 96 h, ii. K₂CO₃, DMF, 50 °C, 48 h, iii. 1-hexanol, 24 h, 160 °C, DBU iv. 1-hexanol, metal salts, 24 h, 160 °C, DBU.

2.4.5. 2,9,16,23-Tetrakis-[3-(diethylamino)phenoxy]-3,10,17,24-tetrachloro-phthalocyaninato}nickel (II) (**8**)

The purification of the crude product was performed by column chromatography on silica gel as the stationary phase using THF as eluent allowed pure compound **8** to be obtained as an isomeric mixture. Yield: 73.5 mg, 72%; IR, γ_{\max} (cm^{-1}): 3076 (C–H, aromatic) 2966–2926 (C–H aliphatic), 1272–1246 (Ar–O–Ar); UV–Vis (CHCl_3): λ_{\max} (nm) ($\log \epsilon$) = 301 (4.89), 677 (5.02); $\text{C}_{72}\text{H}_{64}\text{Cl}_4\text{N}_{12}\text{NiO}_4$ calculated %: C, 63.50; H, 4.74; Cl, 10.41; N, 12.34; O, 4.70; Ni, 4.31; found %: C, 63.58; H, 4.79; N, 12.43; MS: (ESI) yielded an isotopic cluster peak at m/z 1363.14 $[\text{M} + \text{H}]^+$.

2.5. General procedures for quaternized phthalocyanine derivatives (**9–11**)

A mixture of phthalocyanine derivative 0.02 mmol [**5** (27.3 mg), **6** (27.2 mg), **7** (27.4 mg)], 0.0794 mol (5.59 g) of methyl iodide in $5 \text{ cm}^3 \text{ CHCl}_3$ was heated and stirred at 70°C for 5 days in the dark. The resulting green suspension was cooled to ambient temperature and then filtered off. The precipitate was washed with hot CHCl_3

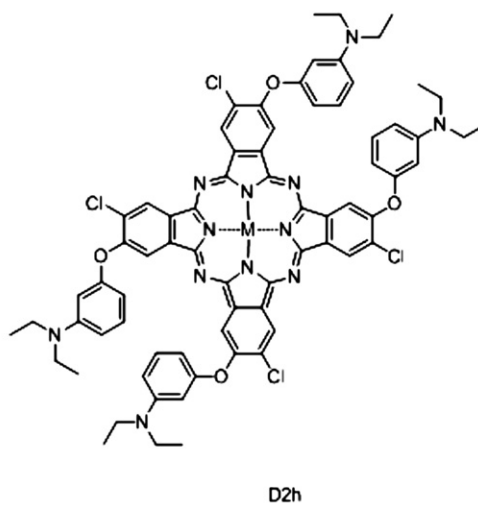
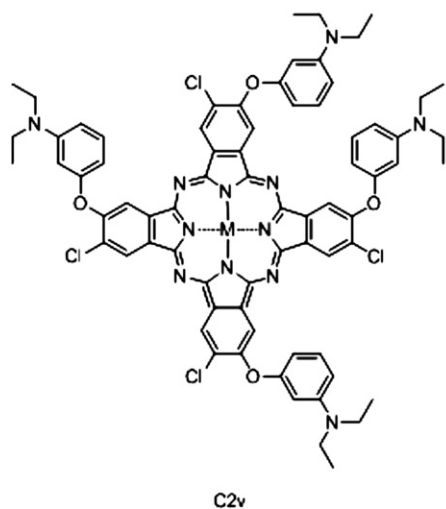
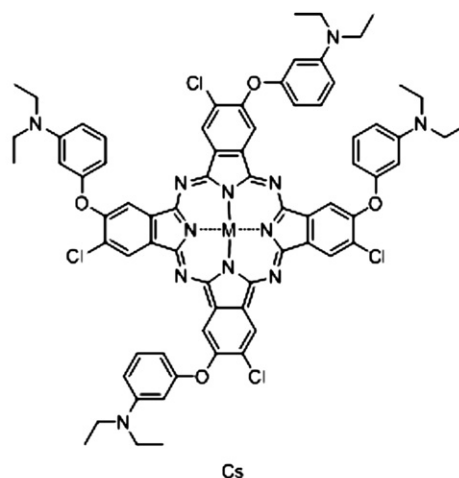
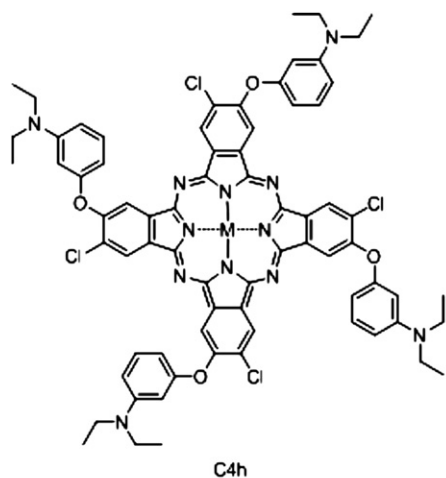
until free any soluble reactant or side product. Finally, quaternized phthalocyanine derivatives were dried *in vacuo*. The colors all of the quaternized phthalocyanines were dark green.

2.5.1. {2,9,16,23-tetrakis-[3-(N,N,N-diethylmethylammonium)phenoxy]-3,10,17,24-tetrachloro-phthalocyaninato}copper (II) iodide (**9**)

Yield: 23.29 mg, 59%; IR γ_{\max} (cm^{-1}) 3018 (C–H, aromatic), 2921–2919 (C–H, aliphatic) 1243–1208 (Ar–O–Ar); UV–Vis (H_2O): λ_{\max} (nm) ($\log \epsilon$) = 335 (4.91), 613 (4.95); $\text{C}_{72}\text{H}_{64}\text{Cl}_4\text{CuN}_{12}\text{O}_4$ calculated% C, 63.27; H, 4.72; Cl, 10.38; N, 12.30; O, 4.68; Cu, 4.65; found %: C, 63.39; H, 4.79; N, 12.43.

2.5.2. {2,9,16,23-tetrakis-[3-(N,N,N-diethylmethylammonium)phenoxy]-3,10,17,24-tetrachloro-phthalocyaninato}cobalt (II)iodide (**10**)

Yield: 24.66 mg, 64%; IR γ_{\max} (cm^{-1}) 3011 (C–H, aromatic), 2976–2941 (C–H, aliphatic), 1244–1209 (Ar–O–Ar); UV–Vis (H_2O): λ_{\max} (nm) ($\log \epsilon$) = 320 (4.91), 619 (5.01); $\text{C}_{76}\text{H}_{76}\text{Cl}_4\text{CoI}_4\text{N}_{12}\text{O}_4$ calculated %: C, 47.30; H, 3.97; Cl, 7.35; I, 26.30; N, 8.71; O, 3.32; Co, 3.05; found %: C, 47.43; H, 4.03; N, 8.83%.



M = 2H(**4**), Cu(**5**), Co(**6**), Zn(**7**), Ni(**8**)

Scheme 2. Isomers of phthalocyanines 4–8.

2.5.3. {2,9,16,23-tetrakis-[3-(*N,N,N*-diethylmethylammonium)phenoxy]-3,10,17,24-tetrachloro-phthalocyaninato}zinc (II)iodide (**11**)

Yield: 24.66 mg, 64%; IR γ_{\max} (cm⁻¹) 3035 (C–H, aromatic), 2976–2941 (C–H, aliphatic) 1244–1203 (Ar–O–Ar); UV–Vis (H₂O): λ_{\max} (nm) (log ϵ) = 341 (5.01), 629 (4.99); C₇₆H₇₆Cl₄I₄·N₁₂O₄Zn calculated %: C, 47.14; H, 3.96; Cl, 7.32; I, 26.22; N, 8.68; O, 3.30; Zn, 3.38; found %: C, 47.28; H, 4.05; N, 8.80%.

3. Results and discussion

3.1. Synthesis and characterization

The first step in the synthesis of the target phthalocyanines **4–8** was to obtain 1-chloro-3,4-dicyano-6-(3-(diethylamino)phenoxy)benzene (**2**). The compound **2** was prepared from 1,2-dichloro-4,5-dicyanobenzene by displacement of the one chloro group of **2** with the OH function of the 3-(diethylamino)phenol at 50 °C in dry DMF under N₂ atmosphere for 96 h (Scheme 1). In the present study, when Na₂CO₃ was used as a base, the chloro groups were partially substituted and 1-chloro-3,4-dicyano-6-(3-(diethylamino)phenoxy)benzene (**2**) was obtained. However, in the case of K₂CO₃, both chloro groups were substituted and 1,2-bis(3-(diethylamino)phenoxy)-4,5-dicyanobenzene (**3**) was obtained. The synthesis of the compound **3** by using K₂CO₃ has recently been described in the literature [38]. The compound **2** was obtained in this study by using Na₂CO₃ because of the probable template effects of K⁺ and Na⁺ ions. [39]. Cyclotetramerization of dinitrile derivative **2** in the presence of 1,8-diazobicyclo[5,4,0]-7-ene and/or anhydrous metal salts [CuCl₂, CoCl₂, Zn(CH₃COO)₂, NiCl₂] at 160 °C in 1-hexanol for 24 h, under a nitrogen atmosphere gave metal-free and metallophthalocyanines (**4–8**), respectively (Scheme 1). Phthalonitrile derivatives containing two different substituted groups afford the isomer mixture of phthalocyanine derivatives. In all cases, a mixture of four possible structural isomers is obtained. We expect that metal-free (**4**) and metallophthalocyanines (**5–8**) were obtained as a statistical mixture of four regioisomers owing to the various possible positions of the diethylaminophenoxy and chloro side-chains relative to one another (Scheme 2). The four probable isomers can be obtained with molecular symmetries (D_{2h}:C_s:C_{2v}:C_{4h} in ratio of 1:1:2:4). To the best of our knowledge, the successful separation of these four isomers with common column chromatography or recrystallization has not been achieved in the literature. No attempt was made to separate the isomers of **4–8**. When the whole molecule is taken into account, it is not possible to define D_{4h} for all the isomers of metallophthalocyanines. Similar argument is also true for the metal-free derivative and describing it with D_{2h} symmetry is ambiguous. Therefore, it should be clear that the products are a mixture of isomers and D_{4h} and D_{2h} symmetry could be pronounced only when the inner phthalocyanine core is taken into account. The newly synthesized phthalocyanines were obtained purely after column chromatography on silica gel by using THF, CHCl₃, CHCl₃/Hexane mixtures as the eluents. These bulky substituents are efficient to hinder the aggregation of macrocycle [14–21,24–27]. The dark green products are extremely soluble in polar and apolar solvents such as CHCl₃, DCM, THF, DMF and DMSO. However the complex **5** is not soluble in DMSO, although others are soluble. Quaternarization of metallophthalocyanines **5–7** was achieved by reaction with excess methyl iodide as quaternarization agent in chloroform as solvent at 70 °C in the dark for 5 days. The hygroscopic phthalocyanine products **9–11** with four quaternary ammonium groups were obtained in high yields (~60%) (Fig. 1). Quaternized products were soluble in water and DMSO, but insoluble in chloroform.

All the synthesized compounds are new except **3**, which was previously reported in the literature [38]. Elemental analysis results and the spectral data (FT-IR ¹H NMR, ESI-MS and UV–Vis) for all new products were consistent with the assigned formulations. IR spectrum of **2** indicated the aromatic C–O–C groups at 1247 cm⁻¹, the C≡N groups at 2236 cm⁻¹, aliphatic groups at 2963–2926 cm⁻¹ and aromatic groups at 3077 cm⁻¹ by intense bands. In addition, the appearance of intense new absorptions at 1272–1247 cm⁻¹ in the spectra attributable to Ar–O–Ar groups confirmed the proposed structure of the compound **2** when compared with the IR spectrum of 1,2-dichloro-4,5-dicyanobenzene (**1**) [25,28,34,35].

After conversion of the dinitrile **2** to the phthalocyanines, the sharp C≡N vibration around 2236 cm⁻¹ disappeared. IR spectra of all the phthalocyanine derivatives showed aromatic C–O–C peaks at 1272–1239 cm⁻¹. The IR spectra of the phthalocyanines **4–8** are very similar, with the exception of the metal-free **4** showing an NH stretching band peak at 3288 cm⁻¹ due to the inner core. The NH proton of metal-free phthalocyanine was also identified in the ¹H NMR spectrum with a broad peak at δ = 5.35 ppm, presenting the typical shielding of inner core protons, which is common feature of the ¹H NMR spectra of metal-free phthalocyanines. No major changes in the IR spectra were found after quaternarization.

¹H NMR spectra of phthalonitrile (**2**), metal-free phthalocyanine (**4**) and the phthalocyanine with diamagnetic metal ion in the core (**7**) were consistent with proposed structures. In the ¹H NMR spectrum of **2** in CDCl₃, the aromatic protons appear as two singlets at 7.87 and 7.13 ppm, two triplets at 7.26 and 6.30 ppm, two doublet doublets at 6.59 and 6.24 ppm. Aliphatic CH₂ and CH₃ protons of ethylaminophenoxy groups appear as a quartet at 3.35 and a triplet at 1.17 ppm, respectively.

The ¹H NMR spectra of **4** and **7** is somewhat broader than the corresponding signals in the dinitrile derivative **2**. It is likely that the broadness results from both chemical exchanges caused by aggregation–disaggregation equilibria and the fact that the obtained product in this reaction is a mixture of four positional isomers which are expected to show chemical shifts only slightly different from each other.

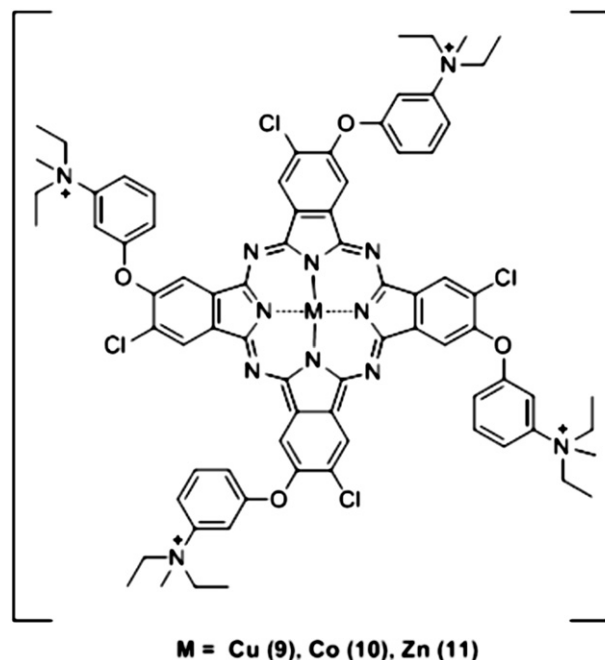


Fig. 1. Quaternized phthalocyanines **9–11**.

3.2. Ground-state electronic absorption spectra

UV–Vis spectra are especially fruitful to establish the structure of the phthalocyanines. The phthalocyanines exhibit typical electronic spectra with two strong absorption regions, one of them is in the visible region at 600–700 nm (Q band) and the other one is in the UV region at about 300–350 nm (B band), both correlate to $\pi-\pi^*$ transitions. Aggregation is usually depicted as a co-planar association of rings progressing from monomer to dimer and higher order complexes and affects the shape of the Q band. Aggregation is dependent on the concentration, nature of the solvent, nature of the substituents, complexed metal ions, and temperature [40]. The ground-state electronic spectra of all metallophthalocyanines (**5–8**) in chloroform display intense Q bands in the visible region around 654–705 nm with relatively sharp absorption peaks and almost no shoulder on the higher energy side, which would correspond to aggregated species and the B bands in the near UV region, around 301–355 nm (Fig. 2) [18,22,28]. In chloroform, the metal-free phthalocyanine (**4**) gives a split Q band in the visible region (670 and 705 nm) as a result of the D_{2h} symmetry [18,27].

UV–Vis spectra of the quaternized metallophthalocyanines (**9–11**) in H_2O show some differences from those of corresponding non quaternized derivatives (**5–8**) in chloroform (Fig. 3). The Q bands are present as a shoulder, while the absorption of the aggregated species is the main band as a result of solvent effect [18].

In this study, the aggregation behavior of **7** was also investigated at different concentrations in chloroform (Fig. 4). As shown in the figure, the Q band increases in intensity with increasing in the concentration of **7** and any new band were observed due to the aggregated species [41,42]. Beer–Lambert Law was obeyed for **7** in the concentrations in the range $4-14 \times 10^{-6} \text{ mol dm}^{-3}$ (Fig. 4).

The electronic absorption of compound **5** and **7** in different organic solvents, such as tetrahydrofuran, dimethyl formamide, chloroform, dimethyl sulfoxide and toluene, are shown in Figs. 5 and 6, respectively. While complex **7** showed aggregation in DMSO, the complex **5** showed aggregation in DCM, DMF, and DMSO. The complex **5** is not soluble in DMSO. To observe the aggregation

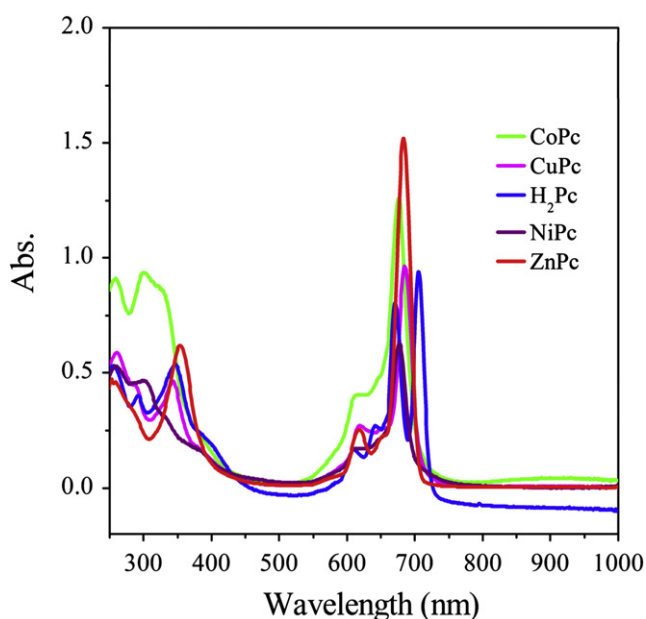


Fig. 2. UV spectra of H_2Pc (**4**), $CuPc$ (**5**), $CoPc$ (**6**), $ZnPc$ (**7**) and $NiPc$ (**8**) ($6 \times 10^{-6} \text{ M}$ in $CHCl_3$).

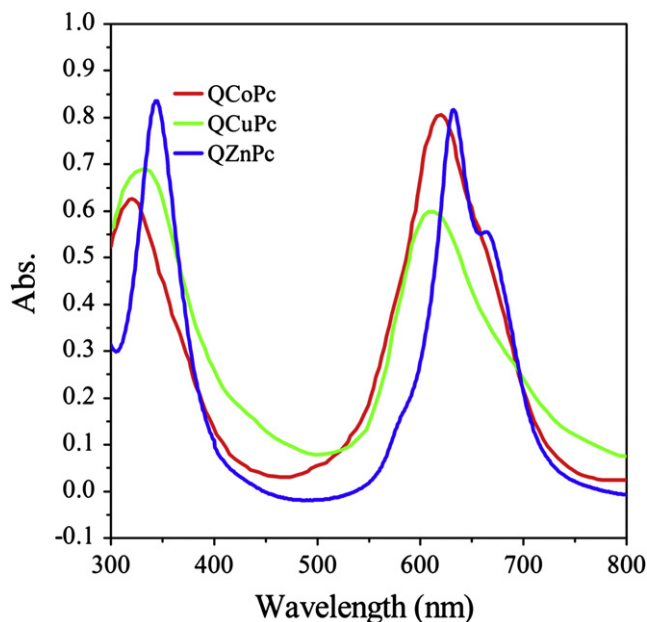


Fig. 3. UV spectra of $QCuPc$ (**9**), $QCoPc$ (**10**) and $QZnPc$ (**11**) ($8 \times 10^{-6} \text{ M}$ in H_2O).

behavior of **5** in DMSO, first of all it was dissolved in DCM, and then DCM was removed by purging with N_2 and then DMSO was added. DMSO solution of the complex **5** was prepared whit this procedure. Fig. 6 (as inset) gives the aggregation behavior of **5** in DMSO at different concentrations. As shown in this figure, the complex **5** aggregates in high extend and the aggregation band at 614 nm is higher than that of the Q band at 685 nm assigned to the monomeric species at all concentrations. It is obvious that the Q band positions of the complexes vary as the solvent is changed. In general, the red shift of the Q band increases with the ascending refractive index of the solvent. In our study, the bathochromic shift of the Q band due to the solvent for compound **7** increased in the following order: tetrahydrofuran < dimethyl formamide < chloroform < dimethyl

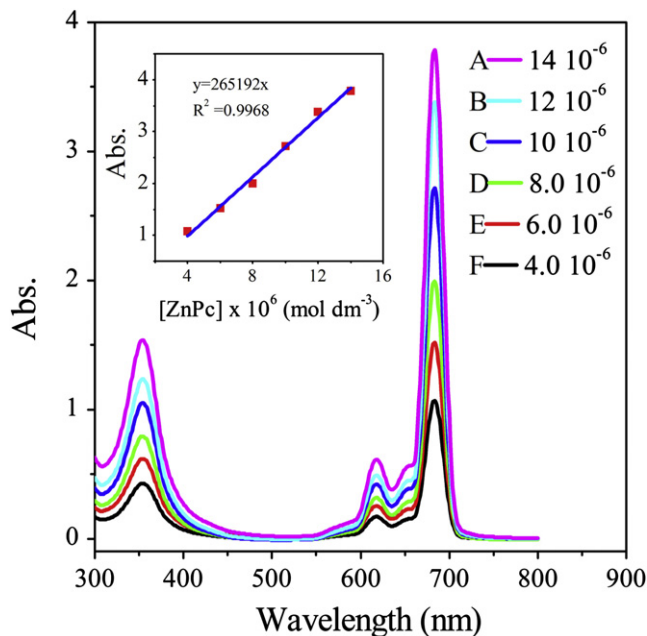


Fig. 4. Absorption spectra of $ZnPc$ (**7**) in $CHCl_3$ at different concentrations: 14×10^{-6} (A), 12×10^{-6} (B), 10×10^{-6} (C), 8×10^{-6} (D), 6×10^{-6} (E) and 4×10^{-6} (F) mol dm^{-3} .

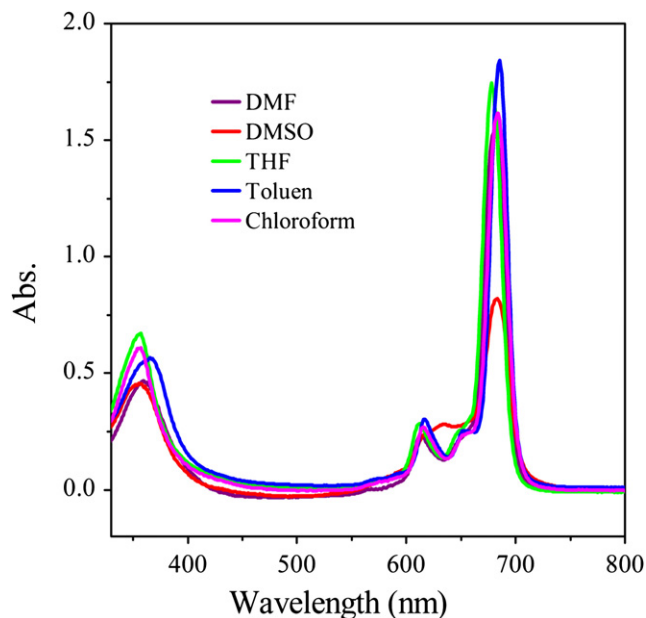


Fig. 5. Absorption spectra of ZnPc (7) in different solvents (6×10^{-6} mol dm^{-3}).

sulfoxide < toluene. The electronic absorption spectra of **7** in these solvents were analyzed by using the method described originally by Bayliss [43]. Fig. 7 displays a plot of the Q band frequency versus the function $(n^2 - 1)/(2n^2 + 1)$, where n is the refractive index of the solvent. The positions of the Q bands in these solvents show almost a linear dependence on this function. This linearity suggests that the shifts are mainly due to the solvation and not to a ligation effect [44].

3.3. Voltammetric characterization

The CVs and SWVs of the phthalocyanines (**H₂Pc (4)**, **CuPc (5)**, **CoPc (6)**, **ZnPc (7)**, and **NiPc (8)**) were obtained in deaerated DCM/

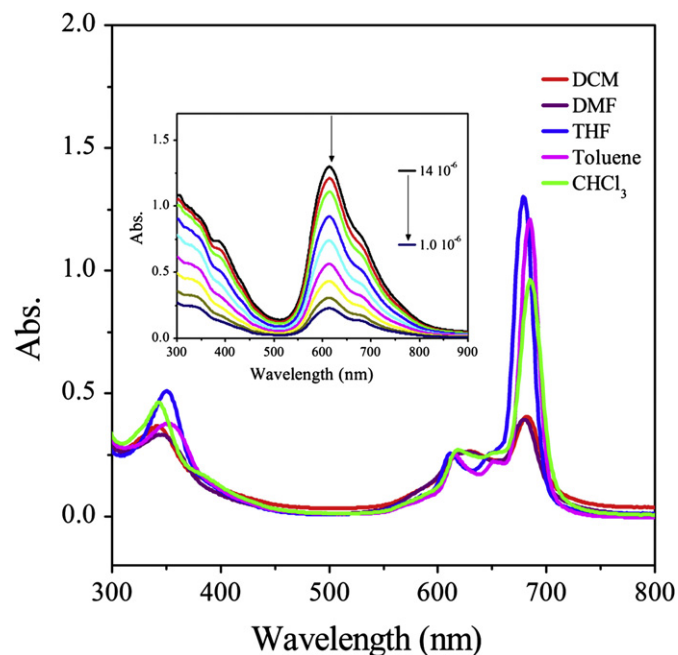


Fig. 6. Absorption spectra of CuPc (5) in different solvents (6×10^{-6} mol dm^{-3}), (inset: absorption spectra of CuPc (5) in DMSO at different concentrations).

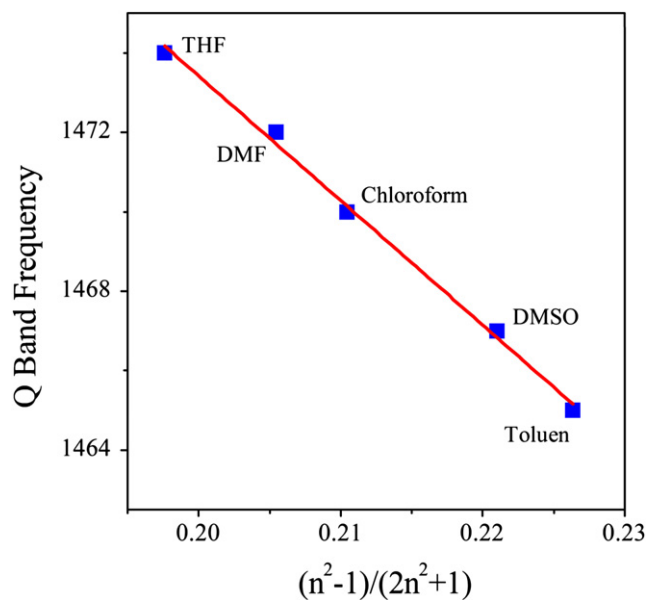


Fig. 7. Plot of the Q band frequency of ZnPc (7) against $(n^2 - 1)/(2n^2 + 1)$, where n is the refractive index of the solvent.

TBAP electrolyte system on a Pt working electrode. Table 1 lists the assignments of the redox couples and estimated electrochemical parameters including the half-wave peak potentials ($E_{1/2}$), ratio of anodic to cathodic peak currents ($I_{p,a}/I_{p,c}$), peak to peak potential separations (ΔE_p), and difference between the first oxidation and reduction processes ($\Delta E_{1/2}$). Peak to peak separations, $E_{1/2}$ and $\Delta E_{1/2}$ values are in agreement with the reported data for redox processes of the metallophthalocyanine complexes [18,45–50]. $\Delta E_{1/2}$ reflects the HOMO–LUMO gap for metal-free Pcs and it is related with HOMO–LUMO gap in MPc species having redox inactive metal center. Presence of four dialkylaminophenoxy substituents on the complexes causes oxidative electro-polymerization of the complexes on the working electrode. When compared with the tetra-substituted dialkylaminophenoxy derivatives of the complexes [38], redox couples of the complexes studied here shift to the negative potentials due to the electron releasing ability of the chloro-substituents. Although the complexes aggregate in less extent and the aggregation changes with the solvent of the complexes, all complexes indicate aggregation behavior in DCM/TBAP electrolyte system during the electrochemical and spectroelectrochemical measurements. This behavior of the complexes may be due to the very high concentration used during electrochemical (5.0×10^{-4} mol dm^{-3}) and spectroelectrochemical (1.0×10^{-3} mol dm^{-3}) measurements. Presence of TBAP salt may also affect the aggregation of the complexes.

Fig. 8 shows the CV and SWV of **H₂Pc (4)**. Within the electrochemical cathodic window of DCM/TBAP in CV measurements; **H₂Pc** illustrates two reversible one-electron reductions at -0.74 and -0.99 V at 0.100 Vs^{-1} scan rate. Third reduction process is recorded at -1.88 V with SWV. For the reduction couples, anodic to cathodic peak separations (ΔE_p) changed from 60 to 125 mV with the scan rates from 10 to 500 mV^{-1} support reversible electron transfer. Reversibility is illustrated by the similarity in the forward and reverse SWVs (Fig. 8b) [51]. Unity of the $I_{p,a}/I_{p,c}$ ratio at all scan rate and linear variation of the $I_{p,c}$ with square root of the scan rates indicated the purely diffusion controlled electron transfer mechanism of the processes. During the anodic CV scans, two intense redox peaks are recorded at 0.94 and 1.13 V. Peak currents of these processes increase with the repetitive CV cycles, while a new redox

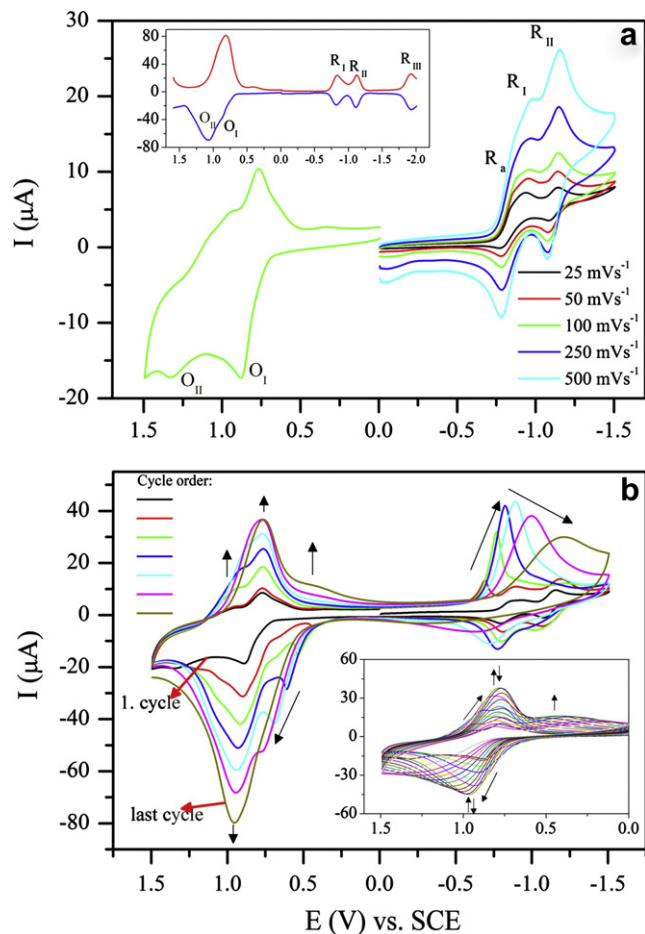


Fig. 9. a) CVs of **CuPc** (5.0×10^{-4} mol dm^{-3}) at various scan rates on Pt in DCM/TBAP; (inset: SWV of **CuPc**, SWV parameters: pulse size = 100 mV; Step Size: 5 mV; Frequency: 25 Hz) b) CVs recorded with repetitive CV cycles within the whole potential window of the electrolyte at 0.100 Vs^{-1} scan rate (inset: CVs recorded with anodic repetitive CV cycles).

reaction; aggregation–disaggregation equilibrium. Second reduction couple is both electrochemically and chemically reversible with respect to the ΔE_p and I_{pa}/I_{pc} ratio change as a function of the scan rate. Reversibility is illustrated by the similarity in the forward and reverse SWVs (Fig. 9a inset) [51]. During the anodic potential scans, **CuPc** electro-polymerizes on the working electrode like **H₂Pc**. (Fig. 9b). Similar voltammetric responses are recorded with all complexes but while polymerization diminishes after the fourth cycle for **H₂Pc**, the process continues until the eighth cycles for **CuPc** and continuously for **ZnPc** and **NiPc**. Changing the potential window of the CV cycles affects the mechanism of the polymerization reaction. When only positive potentials are scanned (Fig. 9b inset), the wave at 0.87 V increases with positive shift as a function of continuous CV cycles. At the same time a new broad wave at around 0.40 V in addition to the waves at 0.90 and 0.77 V are observed with increasing current intensity as a function of CV cycle. However when both the cathodic and anodic potentials are scanned, two extra waves at 0.46 V (with positive shift) and -0.90 V (with negative shift) in addition to other redox processes are recorded (Fig. 9b). These data indicates that polymerization mechanism changes with the potential window of the CV scans. Assignments of the redox couples are performed by spectroelectrochemical measurements given below.

Fig. 10 represents the CV and DPV of **CoPc** (**6**) in DCM/TBAP electrolyte. Within the electrochemical window of DCM/TBAP

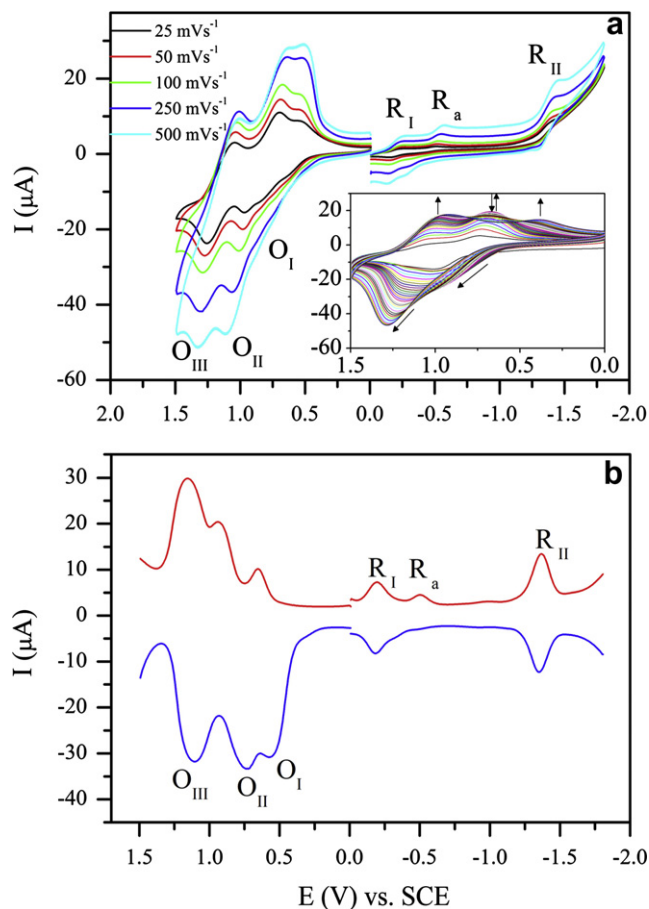


Fig. 10. a) CVs of **CoPc** (5.0×10^{-4} mol dm^{-3}) at various scan rates on Pt in DCM/TBAP (inset: CVs recorded with repetitive CV cycles at 0.100 Vs^{-1} scan rate). b) SWV of **CoPc**, SWV parameters: pulse size = 100 mV; Step Size: 5 mV; Frequency: 25 Hz.

during CV measurements, **CoPc** undergoes two reversible one-electron reduction processes at -0.20 and -1.37 V. For the first reduction couple, the anodic to the cathodic peak separations (ΔE_p) changed from 62 to 115 mV with the scan rates from 10 to 500 mV^{-1} support the reversible electron transfer character of the process. Reversibility is illustrated by the similarity in the forward and reverse SWVs (Fig. 10b) [51]. While the I_{pa}/I_{pc} ratio of first reduction couple is unity at slow scan rates. It deviates from the unity with the increasing scan rates, which indicate existence of a kinetic control after the first reduction process. The wave (R_a) at -0.52 V recorded at high scan rates supports the existence of this kinetic control. While the R_a process is invisible at slow scan rates, its peak current increases more than that of R_I with the increasing scan rates. This wave disappeared with diluting of the solution. These data indicate the aggregation of the complex and aggregated species reduce at -0.52 V. Aggregation–disaggregation equilibrium is affected with the scan rate and concentration; whose responses are recorded as changing in the peak current of the R_a process. Second reduction process has a quasi-reversible electron transfer character. During the anodic scans, similar electro-polymerization process also recorded with **CoPc** like other complexes (Fig. 10a inset). Due to the metal-based oxidation, three oxidation processes are recorded with **CoPc** during the first CV cycle, while there are two waves for other complexes. Polymerization of the complex proceeds continuously and the redox peaks shift to the more positive potential during the continuous cycles. Assignments of the redox couples are performed by spectroelectrochemical measurements given below.

3.4. In-situ spectroelectrochemical measurements

Spectroelectrochemical studies were employed to confirm the assignments in the CVs of the complexes. **H₂Pc**, **ZnPc**, **NiPc**, and **CuPc** have redox inactive Pc centers thus indicate ring-based characters for all redox couples. To represent in-situ spectroelectrochemical response of the metal-free phthalocyanines, spectral changes of **H₂Pc** during the controlled potential application at the redox potentials are given in Fig. 11. For the metal-free phthalocyanines, the symmetry is D_{2h} and therefore there are two sharp bands (split Q band) at 663 and 697 nm [45,48–50,52,53]. Due to the presence of aggregation and/or due to performing the measurements with high concentration, splitting of the Q band is shadowy and an aggregation band is recorded at 663 nm in high intensity. When the working electrode is polarized at -1.00 V, $[\text{H}_2\text{Pc}^{2-}]$ is one-electron reduced to form $[\text{H}_2\text{Pc}^{3-}]^{1-}$ anion. During the reduction of $[\text{H}_2\text{Pc}^{2-}]$ at constant potential application, a sharp single band is recorded at 677 nm instead of the split Q band. At the same time, a new band is recorded at 400 nm, while the intensity of the B band decreases with shifting from 334 to 341 nm (Fig. 11a). During this process, well-defined isosbestic points are recorded at 278, 350, 476, 654, and 697 nm, which demonstrate that the reduction proceeds cleanly in deoxygenated DCM to give a single, reduced species. Rollmann and Iwamoto [53] and Koca et al. [18,54] also reported similar spectroscopic changes for one-electron reduction of **H₂Pc** complexes. It was mentioned that there might be a symmetry change from D_{2h} to D_{4h} because of the substitution of central hydrogens by the cations of supporting electrolyte. It was shown that the pair of excited states which usually give rise to the Q band doubling in the $[\text{H}_2\text{Pc}^{3-}]^{1-}$ species, is still present but the states are too close together to be resolved. During the potential application at -1.20 V, $[\text{H}_2\text{Pc}^{3-}]^{1-}$ is one-electron reduced to form $[\text{H}_2\text{Pc}^{4-}]^{2-}$ dianion (Fig. 11b). Spectroscopic changes show a band, which tries to increase at around 510 nm. But due to the decomposition of the reduced species, all band decreases in intensity. During the oxidation of **H₂Pc** at 1.20 V applied potential, intensity of all bands decrease in intensity (Fig. 11c). These spectroscopic changes may due to the electro-polymerization of the complex on the working electrode which diminishes concentration of the species in the bulk solution. The color of the neutral **H₂Pc** was recorded as greenish blue ($x = 0.2597$ and $y = 0.3445$). Instinct color changes were not recorded between the electrogenerated forms of the complexes.

Fig. 12 shows the spectral changes of **CuPc** as a representative of MPC's having redox inactive metal center under applied potential. Before any potential application, the band at 626 nm results from the aggregated species, which support the aggregation–disaggregation equilibrium recorded by the CV and SWV measurements. Under open-circuit potential, an intense aggregation band is recorded at 626 nm in addition to the common Q band at 677 nm and the B band at 330 nm in the spectra of the complex. During the controlled potential reductions of **CuPc** at -0.90 V potential applications, two distinct spectral changes are recorded. First of all, while the Q band at 677 nm decreases in intensity, the band assigned to the aggregated species increases due to the shifting of the aggregation–disaggregation equilibrium under applied potential (from red to black spectrum in Fig. 12a). At the same time, new bands at 587 and 950 nm are recorded. Then while the Q band and the band at 626 nm decrease in intensity, a new band is recorded at 576 nm potential (from black to blue spectrum in Fig. 12a). During this electrochemical reduction, isosbestic points are observed at around 320, 438, and 757 nm with oscillation, and various isosbestic points at around 500 nm are recorded. These data demonstrates that the reduction process gives more than a single product, which may be reduced, aggregated and disaggregated

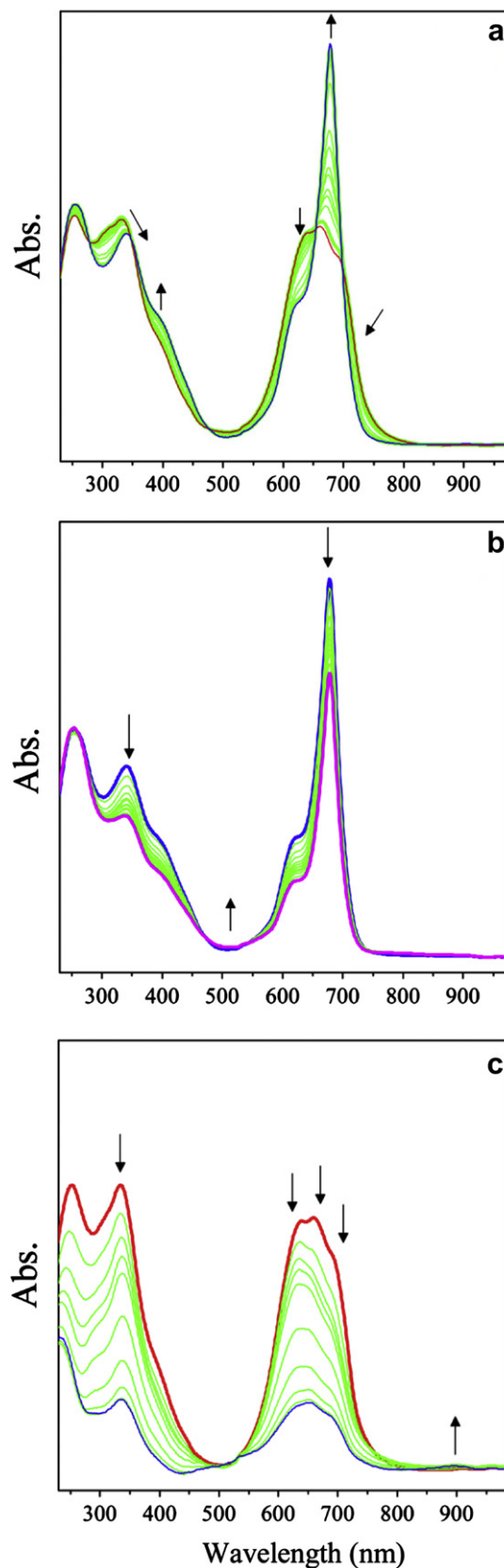


Fig. 11. In-situ UV–vis spectral changes of **H₂Pc**. a) $E_{\text{app}} = -0.50$ V b) $E_{\text{app}} = -1.50$ V c) $E_{\text{app}} = 0.70$ V.

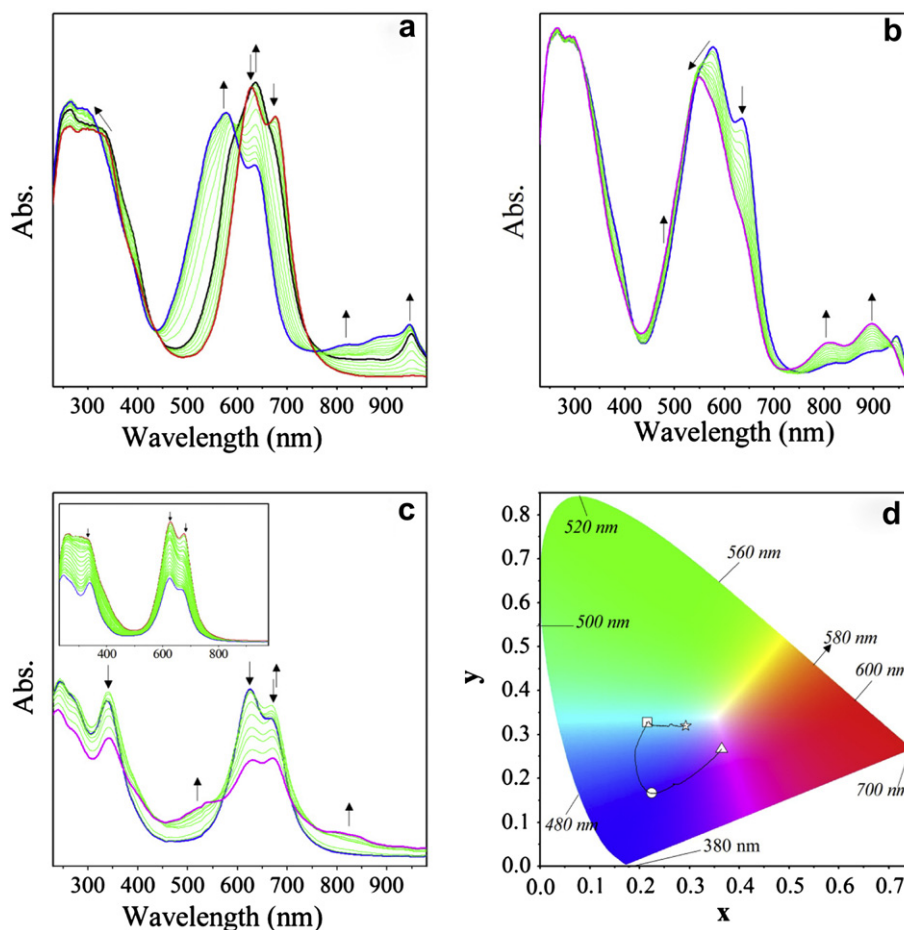


Fig. 12. In-situ UV–vis spectral changes of **CuPc**. a) $E_{app} = -0.50$ V b) $E_{app} = -1.50$ V c) Initial part of the spectral changes at $E_{app} = 0.70$ V (inset: final part of the spectral changes at $E_{app} = 0.70$ V). d) Chromaticity diagram of **CuPc**. (Each symbol represents the color of electrogenerated species; \square : $[\text{Cu}^{\text{II}}\text{Pc}^{-2}]$, \circ : $[\text{Cu}^{\text{II}}\text{Pc}^{-3}]^{-1}$, \triangle : $[\text{Cu}^{\text{II}}\text{Pc}^{-3}]^{-2}$; $[\text{Cu}^{\text{II}}\text{Pc}^{-1}]^{+1}$).

copper(I) species. However, general trend of the spectroscopic changes indicates a Pc ring reduction process and assigns the first reduction process (couple R_1) to $[\text{Cu}^{\text{II}}\text{Pc}^{-2}]/[\text{Cu}^{\text{II}}\text{Pc}^{-3}]^{-1}$ process [46,49,55–57]. Spectroscopic changes under controlled potential application at -1.20 V support the further reduction of the monoanionic $[\text{Cu}^{\text{II}}\text{Pc}^{-3}]^{-1}$ species to $[\text{Cu}^{\text{II}}\text{Pc}^{-4}]^{-2}$ (Fig. 12b). Decreasing of the Q band intensity without shift and observation of new bands at 536, 800, and 897 nm are characteristics of the ring reduction process. During the oxidation of **CuPc** (Fig. 12c inset) at 0.90 V, the absorption of all band decrease in intensity which indicates the polymerization of the complex on the working electrode. Under applied potential at 1.30 V, the Q band at 677 nm and its shoulder at 627 nm decrease in intensity without shift, while new bands at 525 and 825 nm appears with increasing in intensity (Fig. 12c). These changes are typical of the ring-based oxidation and assigned to $[\text{Cu}^{\text{II}}\text{Pc}^{-2}]/[\text{Cu}^{\text{II}}\text{Pc}^{-1}]^{+1}$ process [46,49,55–57].

The color change of the complexes during the redox processes were recorded using in-situ colorimetric measurements. Without any potential application, the solution of **CuPc** is greenish blue ($x = 0.2158$ and $y = 0.3273$) (Fig. 12d). As the potential is stepped from 0 to -0.90 V, the color of the neutral $[\text{Cu}^{\text{II}}\text{Pc}^{-2}]$ start to changes and dark blue color ($x = 0.2244$ and $y = 0.1664$) of monoanionic form of $[\text{Cu}^{\text{II}}\text{Pc}^{-3}]^{-1}$ is obtained at the end of the first reduction. Similarly color of the dianionic species, $[\text{Cu}^{\text{II}}\text{Pc}^{-4}]^{-2}$ is recorded as purple ($x = 0.3648$ and $y = 0.2666$). Monocationic species, $[\text{Cu}^{\text{II}}\text{Pc}^{-1}]^{+1}$ has light violet color ($x = 0.2927$ and $y = 0.319$).

Fig. 13 represents in-situ UV–vis spectral changes and in-situ recorded chromaticity diagram of **CoPc** (**6**) in DCM/TBAP during the potential application at the potentials of the redox processes. Before any potential application, an aggregation band is recorded at 626 nm in addition to the Q band of the monomeric species at 670 nm. During the first reduction process, two different spectral changes are recorded. First of all, due to the change in the aggregation–disaggregation equilibrium, a single broad band is recorded at 655 nm instead of the bands at 626 and 670 nm. At the same time a new band starts to increase at 474 nm. These spectral changes support the reduction of the aggregated species. Then while the band at 655 nm shifts to 706 nm, the new band at 474 nm enhances in current intensity. These spectral changes indicated the metal-based reduction of both monomeric **CoPc** species and characterize formation of the $[\text{Co}^{\text{I}}\text{Pc}^{-2}]^{1-}$ species under the applied potential at -0.40 V (Fig. 13a) [54–60]. This process gives a color changes from blue ($x = 0.2117$ and $y = 0.2852$) to greenish yellow ($x = 0.3798$ and $y = 0.3984$) as shown in the chromaticity diagram (Fig. 13d). As shown in Fig. 13b, the Q band at 706 nm decreases without shift while a new broad band is recorded at 544 nm under the controlled potential application at -1.40 V. These spectral changes are characteristic of the ring-based reduction of $[\text{Co}^{\text{I}}\text{Pc}^{-2}]^{1-}$ species to $[\text{Co}^{\text{I}}\text{Pc}^{-3}]^{2-}$ species. Fig. 13c represents the spectral changes during the first oxidation process of the complex. During 0.80 V potential application, while the intensity of the Q band increases, the band at 626 nm decreases in intensity. At the same time a new band is recorded at 370 nm. These spectral

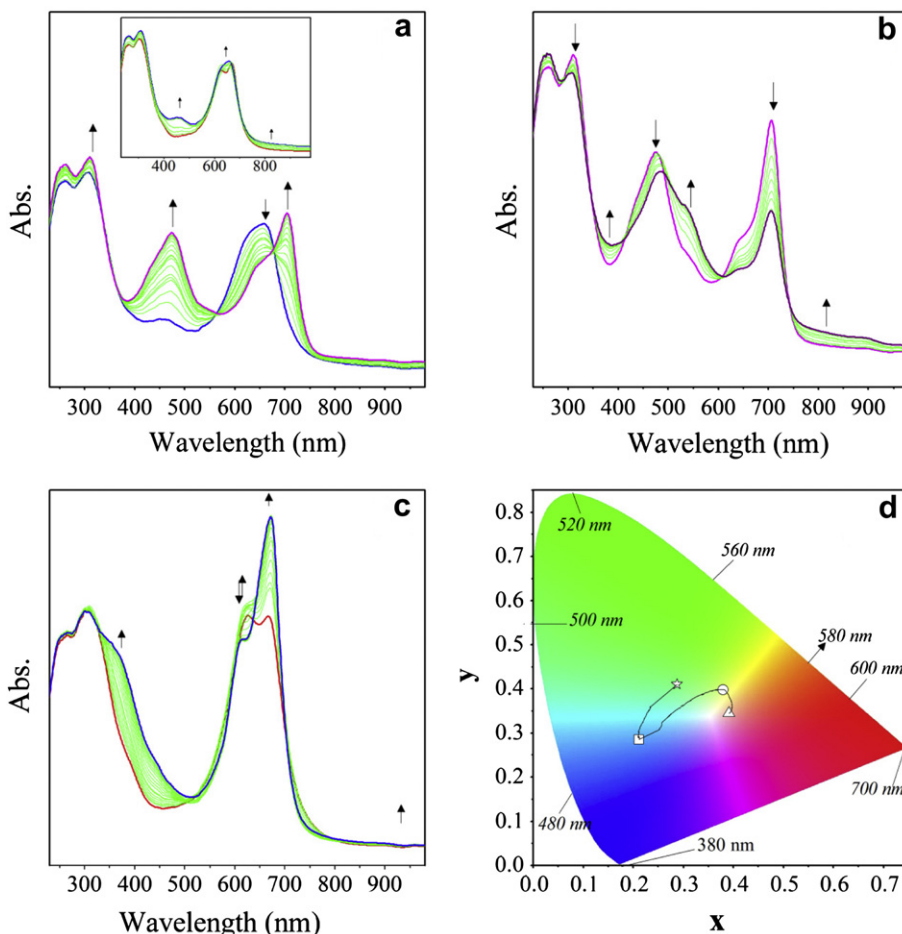


Fig. 13. In-situ UV-vis spectral changes of CoPc. a) Final part of the spectral changes at $E_{app} = -0.50$ V (Initial part of the spectral changes at $E_{app} = -0.50$ V). b) $E_{app} = -1.50$ V c) $E_{app} = 1.00$ V d) Chromaticity diagram of CoPc. (Each symbol represents the color of electrogenerated species; \square : $[\text{Co}^{\text{II}}\text{Pc}^{-2}]$, \circ : $[\text{Co}^{\text{I}}\text{Pc}^{-2}]^{-1}$, \triangle : $[\text{Co}^{\text{I}}\text{Pc}^{-3}]^{-2}$, \star : $[\text{Co}^{\text{II}}\text{Pc}^{-1}]^{+1}$).

changes indicate the ligand-based process and changing of the aggregation–disaggregation equilibrium during the oxidation process. Under applied potential at 1.30 V, intensity of all bands decreased, which supports electro-polymerization of the complex on the working electrode. Color changes during the reduction and oxidation processes are represented in Fig. 13d.

4. Conclusion

As seen in Scheme 1, the reaction between 1,2-dichloro-4,5-dicyanobenzene and 3-(diethylamino)phenol in the presence of Na_2CO_3 as a base gives the compound **2** which is contrary to the compound **3** obtained using K_2CO_3 . This work has also presented a comprehensive investigation of solvent effects on the aggregation of this octa-substituted zinc phthalocyanine complex. The aggregation properties are studied for zinc and copper phthalocyanines in tetrahydrofuran, dimethyl formamide, chloroform, dimethyl sulfoxide, dichloromethane and toluene. The effect of the concentration on the aggregation properties for complex **7** was also studied in chloroform. No aggregation was demonstrated in chloroform from concentration between 14×10^{-6} and 4×10^{-6} mol dm^{-3} . Voltammetric and spectroelectrochemical studies show that while H, Zn, Ni and Cu phthalocyanines give ring-based, multi-electron and reversible/*quasi*-reversible reduction processes, complexes electro-polymerize on the working electrode during oxidation reactions. Similarly cobalt phthalocyanine gives both metal and ring-based, diffusion controlled, multi-electron and reversible/*quasi*-reversible

reduction processes and electro-polymerizes during the anodic scans. Definite determination of the colors of the electrogenerated anionic and cationic form of the complexes is important to decide the possible electrochromic application of the complexes.

Acknowledgements

This work was supported by the Research Fund of the Istanbul Technical University and TUBITAK (Project no. 109T163).

References

- [1] Leznoff CC, Lever ABP. Phthalocyanines properties and applications, vols. 1–4. Weinheim: VCH; 1989–1996.
- [2] McKeown NB. Phthalocyanine materials. Synthesis, structure and function. Cambridge University Press; 1998.
- [3] Kadish K, Smith KM, Guillard R, editors. The porphyrin handbook, vols. 15–20. Boston: Academic Press; 2003.
- [4] Lawrence E, Patonay G. Effects of organic and aqueous solvents on the electronic absorption and fluorescence of chloroaluminum (III) tetrasulphonated naphthalocyanine. *Talanta* 1999;48:933–42.
- [5] Hoffman JW, Zealand F, Turker S. Peripheral and axial substitution of phthalocyanines with solketal groups: synthesis and in vitro evaluation for photodynamic therapy. *J Med Chem* 2007;50(7):1485–94.
- [6] Bonnet R, Martinez G. Photobleaching of sensitizers used in photodynamic therapy. *Tetrahedron* 2001;57:9513–47.
- [7] Kolarova H, Nevrelva P, Bajgar R. In vitro photodynamic therapy on melanoma cell lines with phthalocyanine. *Toxicol In Vitro* 2007;21:249–53.
- [8] Macdonald IJ, Dougherty TJ. Basic principles of photodynamic therapy. *J Porphyrins Phthalocyanines* 2001;5:105–29.

- [9] Sakamoto K, Kato T, Ohno-Okumura E, Watanabe M, Cook MJ. Synthesis of novel cationic amphiphilic phthalocyanine derivatives for generation photosensitizer using photodynamic therapy of cancer. *Dyes Pigm* 2005;64:63–71.
- [10] Ogunsiye A, Nyokong T. Photophysical and photochemical studies of sulfonated non-transition metal phthalocyanines in aqueous and non-aqueous media. *J Photochem Photobiol, A* 2005;173:211–20.
- [11] Alvarez-Mico X, Calvete MJF, Hanack M, Ziegler T. The first example of anomeric glycoconjugation to phthalocyanines. *Tetrahedron Lett* 2003;47:3283–6.
- [12] Riberio AO, Tome JPC, Neves MGPMS, Tome NAC, Cavaleiro JAS, Serra OA, et al. [1,2,3,4-Tetrakis(α/β -d-galactopyranos-6-yl)phthalocyaninato]-zinc(II). *Tetrahedron Lett* 2006;47:9177–80.
- [13] Kazuo O, Shun-Ichiro O, Okura I. Preparation of a water-soluble fluorinated zinc phthalocyanine and its effect for photodynamic therapy. *J Photochem Photobiol, B* 2000;59:20–5.
- [14] Koçak M, Gürek A, Gül A, Bekaroğlu O. Synthesis and characterization of phthalocyanines containing 4 14-membered tetraaza macrocycles. *Chem Ber* 1994;127:355.
- [15] Koçak M, Okur Aİ, Bekaroğlu Ö. Novel 2-Fold-Macrocycle-Substituted phthalocyanines. *J Chem Soc Dalton Trans* 1994;3:323–6.
- [16] Koçak M, Cihan A, Okur Aİ, Gül A, Bekaroğlu Ö. Novel crown ether-substituted phthalocyanines. *Dyes Pigm* 2000;45:9–14.
- [17] Şener MK, Gül A, Koçak MB. Synthesis of tetra(tricarboxy)- and tetra(dicarboxy)-substituted soluble phthalocyanines. *J Porphyrins Phthalocyanines* 2003;7:617–22.
- [18] Atsay A, Koca A, Koçak MB. Synthesis, electrochemistry and in situ spectroelectrochemistry of water soluble phthalocyanines. *Transition Met Chem* 2009;34:877–90.
- [19] Yenilmez Y, Okur Aİ, Gül A. Peripherally tetra-Palladated phthalocyanines. *J Org Chem* 2007;69:940–5.
- [20] Şener MK, Koca A, Gül A, Koçak MB. Novel phthalocyanines with naphthalenic substituents. *Transition Met Chem* 2008;33:867–72.
- [21] Şener MK, Koca A, Gül A, Koçak MB. Synthesis and electrochemical characterization of biphenyl-malonic ester substituted cobalt, copper and palladium phthalocyanines. *Polyhedron* 2007;26:1070–6.
- [22] Hamuryudan E. Synthesis and solution properties of phthalocyanines substituted with four crown ethers. *Dyes Pigm* 2006;68(2–3):151–7.
- [23] Meray Ş, Bekaroğlu Ö. Synthesis and characterization of novel phthalocyanines with four tridentate NNS substituents and four chloro groups. *J Chem Soc Dalton Trans* 1999;24:4503–10.
- [24] Hamuryudan E, Meray Ş, Bayır ZA. Synthesis of phthalocyanines with tridentate branched bulky and alkylthio groups. *Dyes Pigm* 2003;59:235–42.
- [25] Ogunsiye A, Durmus M, Atilla D, Gürek AG, Ahsen V, Nyokong T. Synthesis, photophysical and photochemical studies on long chain zinc phthalocyanine derivatives. *Synth Met* 2008;158:839–47.
- [26] Dinçer HA, Gül A, Koçak MB. A novel route to 4-chloro-5-alkyl phthalonitrile and phthalocyanines derived from it. *J Porphyrins Phthalocyanines* 2004;8:1204–8.
- [27] Dinçer HA, Gül A, Koçak MB. Tuning of phthalocyanine absorption ranges by additional substituents. *Dyes Pigm* 2007;74:545–50.
- [28] Dinçer HA, Koca A, Gül A, Koçak MB. Novel phthalocyanines bearing both quaternizable and bulky substituents. *Dyes Pigm* 2008;76:825–31.
- [29] Burat AK, Koca A, Lewtack JP, Gryko DT. Synthesis, physicochemical properties and electrochemistry of morpholine-substituted phthalocyanines. *J Porphyrins Phthalocyanines* 2010;14:605–14.
- [30] Arslanoğlu Y, Hamuryudan E. Synthesis and derivatization of near-IR absorbing titanylphthalocyanines with dimethylaminoethylsulfanyl substituents. *Dyes Pigm* 2007;75:150–5.
- [31] Ertem B, Bilgin A, Gök Y, Kantekin H. The synthesis and characterization of novel metal-free and metallophthalocyanines bearing eight 16-membered macrocycles. *Dyes and Pigm* 2008;77:537–44.
- [32] Bayır ZA. Synthesis and characterization of novel soluble octa-cationic phthalocyanines. *Dyes Pigm* 2005;65:235–42.
- [33] Dabak S, Gümüç G, Gül A, Bekaroğlu Ö. Synthesis and properties of new phthalocyanines with tertiary or quaternized aminoethylsulfanyl substituents. *J Coord Chem* 1996;38:287–93.
- [34] Gürsoy S, Cihan A, Koçak MB, Bekaroğlu Ö. Synthesis and complexation of a novel soluble vic-dioxime ligand. *Monatsh Chem* 2001;132:813–9.
- [35] Karaoğlu HRP, Gül A, Koçak MB. Synthesis and characterization of a new tetra-cationic phthalocyanine. *Dyes and Pigm* 2008;76:231–5.
- [36] Sesalan BŞ, Koca A, Gül A. Water soluble novel phthalocyanines containing dodeca-amino groups. *Dyes and Pigm* 2008;79:259–64.
- [37] Wöhrle D, Eskes M, Shigehara K, Yamada A. A simple synthesis of 4,5-disubstituted 1,2-dicyanobenzenes and 2,3,9,10,16,17,23,24-octasubstituted phthalocyanines. *Synthesis* 1993;2:194–6.
- [38] Dei D, Chiti G, De Filippis MP, Fantetti L, Giuliani F, Giuntini F, et al. Phthalocyanines as photodynamic agents for the inactivation of microbial pathogens. *J Porphyrins Phthalocyanines* 2006;10:147–59.
- [39] Gürek AG, Bekaroğlu Ö. Dioxo-dithia macrocycle-bridged dimeric with hexakis (alkylthio)-substituents and network polymer phthalocyanines. *J Porphyrins Phthalocyanines* 1997;1:67–76.
- [40] Engelkamp H, Nolte RJM. Molecular materials based a crown ether functionalized phthalocyanines. *J Porphyrins Phthalocyanines* 2000;4:454–9.
- [41] Simon J, Bossoul P. In: Leznoff CC, Lever ABP, editors. *Phthalocyanines: properties and applications*, vol. 2. New York: VCH Publishers; 1993. p. 223.
- [42] Özcesmeci M, Özcesmeci İ, Hamuryudan E. Synthesis and characterization of new polyfluorinated dendrimeric phthalocyanines. *Polyhedron* 2010;29:2710–5.
- [43] Bayliss NS. The effect of the electrostatic polarization of the solvent on electronic absorption spectra in solution. *J Chem Phys* 1950;18:292–6.
- [44] Law WF, Liu RCW, Jiang JH, Ng DKP. Synthesis and spectroscopic properties of octasubstituted (phthalocyaninato)titanium(IV) complexes. *Inorg Chim Acta* 1997;256:147–50.
- [45] Lever ABP, Milaeva ER, Speier G. The redox chemistry of metallophthalocyanines in solution. In: Leznoff CC, Lever ABP, editors. *Phthalocyanines: properties and applications*, vol. 3. New York: VCH; 1993. p. 5–27.
- [46] Günsel A, Kandaz M, Koca A, Salih B. Functional fluoro substituted tetrakis-metallophthalocyanines: synthesis, spectroscopy, electrochemistry and spectroelectrochemistry. *J Fluor Chem* 2008;129:662–8.
- [47] Özer M, Altındal A, Özkaya AR, Bulut M, Bekaroğlu Ö. Synthesis, characterization and some properties of novel bis(pentafluorophenyl)methoxyl substituted metal free and metallophthalocyanines. *Polyhedron* 2006;25:3593–602.
- [48] Li R, Zhang X, Zhu IP, Ng DKP, Kobayashi N, Jiang J. Electron-donating or -withdrawing nature of substituents revealed by the electrochemistry of metal-free phthalocyanines. *Inorg Chem* 2006;45:2327–34.
- [49] Simicglavaski B, Zecevic S, Yeager EJ. Spectroelectrochemical insitu studies of phthalocyanines. *J Electrochem Soc* 1987;134:C130.
- [50] Alemdar A, Özkaya AR, Bulut M. Synthesis, spectroscopy, electrochemistry and in situ spectroelectrochemistry of partly halogenated coumarin phthalonitrile and corresponding metal-free, cobalt and zinc phthalocyanines. *Polyhedron* 2009;28:3788–96.
- [51] Kissinger PT, Heineman WR. *Laboratory techniques in electroanalytical chemistry*. 2nd ed. New York: Marcel Dekker; 1996. pp. 51–163.
- [52] Acar I, Bıyıklıoğlu Z, Koca A, Kantekin H. Synthesis, electrochemical, in situ spectroelectrochemical and in situ electrochromic characterization of new metal-free and metallophthalocyanines substituted with 4-{2-[2-(1-naphthyl)ethoxy]ethoxy} groups. *Polyhedron* 2010;29:1475–84.
- [53] Rollmann LD, Iwamoto RT. Electrochemistry, electron paramagnetic resonance, and visible spectra of cobalt, nickel, copper, and metal-free phthalocyanines in dimethyl sulfoxide. *J Am Chem Soc* 1968;90:1455–63.
- [54] Koca A, Özkaya AR, Selçukoğlu M, Hamuryudan E. Electrochemical and spectroelectrochemical characterization of the phthalocyanines with pentafluorobenzyloxy substituents. *Electrochim Acta* 2007;52:2683–90.
- [55] Agboola B, Ozoemena KI, Nyokong T. Synthesis and electrochemical characterisation of benzylmercapto and dodecylmercapto tetra substituted cobalt, iron, and zinc phthalocyanines complexes. *Electrochim Acta* 2006;51:4379–87.
- [56] Kulaç D, Bulut M, Altındal A, Özkaya AR, Salih B, Bekaroğlu Ö. Synthesis and characterization of novel 4-nitro-2-(octyloxy)phenoxy substituted symmetrical and unsymmetrical Zn(II), Co(II) and Lu(III) phthalocyanines. *Polyhedron* 2007;26:5432–40.
- [57] Koca A, Bayar Ş, Dinçer HA, Gonca E. Voltammetric, in-situ spectroelectrochemical and in-situ electrochromic characterization of phthalocyanines. *Electrochim Acta* 2009;54:2684–92.
- [58] Nombona N, Nyokong T. The synthesis, cyclic voltammetry and spectroelectrochemical studies of Co(II) phthalocyanines tetra-substituted at the alpha and beta positions with phenylthio groups. *Dyes Pigm* 2009;80:130–5.
- [59] Mbambisa G, Tau P, Antunes E, Nyokong T. Synthesis and electrochemical properties of purple manganese(III) and red titanium(IV) phthalocyanine complexes octa-substituted at non-peripheral positions with pentylthio groups. *Polyhedron* 2007;26:5355–64.
- [60] Koca A, Özçesmeci M, Hamuryudan E. Substituents effects to the electrochemical, and in situ spectroelectrochemical behavior of metallophthalocyanines: electrocatalytic application for hydrogen evolution reaction. *Electroanalysis* 2010;22:1623–33.